Impurity Effects at Hydrophobic Surfaces

Yuki Uematsu
Department of Chemistry, Kyushu University, Fukuoka 819-0395, Japan

Douwe Jan Bonthuis and Roland R. Netz
Fachbereich Physik, Freie Universität Berlin, 14195 Berlin, Germany
(Dated: September 8, 2018)

The effective charge of hydrophobic surfaces and in particular of the air-water interface is a crucial parameter for electrochemistry, colloidal chemistry and interfacial science, but different experiments give conflicting estimates. Zeta-potential and disjoining-pressure measurements point to a strongly negative surface charge, often interpreted as being due to adsorbing hydroxide ions. In contrast, surface tension measurements of acids and bases suggest the hydronium ion to be surface active, in agreement with some surface-specific non-linear spectroscopy results. The air-electrolyte interfacial tension exhibits a characteristic minimum at millimolar electrolyte concentration for all salts, the so-called Jones-Ray effect, which points to competitive adsorption mechanisms present in dilute electrolyte solutions. We show that all these puzzling experimental findings can be explained by the presence of trace amounts of surface-active charged impurities, most likely anionic surfactants.

INTRODUCTION

The interface between electrolytes and air, oil or other hydrophobic materials is a very popular experimental model system since it lacks complications due to dissociable surface groups. Consequently, it has been intensely investigated in studies of the surface tension [1–6] and its dynamics [7, 8], zeta potential [9–12], bubble coalescence [13, 14], stability of nano-bubbles [15–17], and disjoining pressure [18–21]. Although the air-electrolyte interface is the simplest possible electrochemical system, its effective surface charge is still debated [22–33]. Since a long time it has been known that the electrophoretic mobility of gas bubbles in pure water is negative, which led to the conclusion that OH^- ions adsorb at the air-water interface [9, 10]. The negative sign of the air-water interface charge is also supported by the stability of thin water films on negatively charged silica surfaces [18–21], whereas surface-sensitive nonlinear spectroscopy suggests H_3O^+ ions to be present at the air-water interface [22, 23] instead. From the molecular modeling side, the situation is also not clear; some simulations support hydroxide adsorption [25, 28] and others not [24, 29–32]. So while the interface between electrolytes and hydrophobic surfaces is conceptually simple, its basics properties seem surprisingly complex. This review summarizes puzzling experimental measurements of the surface tension, the zeta potential, and the disjoining pressure of electrolyte-hydrophobe interfaces and provides an interpretation in terms of the presence of trace amounts of charged surface-active impurities.

ELECTROLYTE SURFACE TENSION

Basic insight is provided by surface tension studies of the air-electrolyte interface. The Gibbs adsorption isotherm,

$$d\gamma = -\sum_i \Gamma_i d\mu_i, \tag{1}$$

relates the change of the surface tension γ to the sum of the surface excesses of molecules of type i multiplied by changes of the respective chemical potentials μ_i. Fig. 1a shows the experimental surface tension increment $\Delta\gamma$ [1, 3] as a function of added salt concentration $c^{\rm b}_{\rm salt}$ together with linear fits according to $\Delta\gamma = Ac^{\rm b}_{\rm salt}$ [3, 4, 14]. Most salts, except the acids, increase the surface tension in an ion-specific fashion. For ideal solutions Eq. (1) predicts the total ionic surface excess to be proportional to $-A$; Fig. 1a thus implies that most ions are repelled from the interface while acids exhibit a net attraction. The ionic repulsion from the air-electrolyte interface is partly due to dielectric image charge repulsion [2], while the ion specificity is caused by interfacial hydration effects [36].

Fig. 1b shows the experimental coefficients A of different electrolytes [4, 14] sorted in columns with respect to the anionic surface affinity, which increases according to the Hofmeister series (from left to right) and basically reflects the anion size (with OH^- constituting a noteworthy and debated anomaly). The surface affinities of the cations are rather similar, except for H_3O^+, which stands out and gives rise to a net positive interface excess for all anions (except in combination with OH^- where the surface affinity is zero by virtue of chemical equilibrium). Neglecting correlated adsorption of H_3O^+ with anions and incomplete acid dissociation at surfaces [37], this suggests that H_3O^+ has a strong affinity to the air-water interface, while OH^- is repelled. This contrasts with many other interpretations [24–28, 30–33, 37], so microscopic insight is direly needed.

Figs. 2a/c show snapshots of force-field based molecular dynamics simulations of HCl and NaOH solution-air interfaces and Figs. 2b/d present the extracted poten-

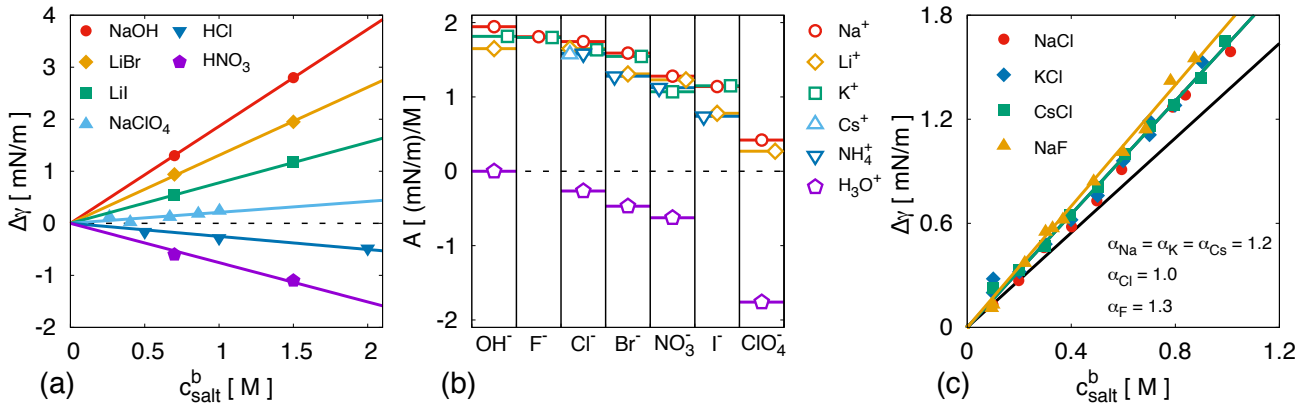

FIG. 1. (a) Surface tension increment of different electrolyte solutions with respect to pure water at relatively large salt concentrations, the lines are linear fit functions according to $\Delta\gamma = Ac^{\mathrm{b}}_{\mathrm{salt}}$. The experimental data of NaOH, LiBr, LiI, HCl, and HNO_3 are taken from Ref. 1, whereas the data of $NaClO_4$ is taken from Ref. 3. (b) Experimental linear coefficients A are sorted with respect to the anions [4, 14]. Anions exhibits pronounced ion specificity according to the anionic Hofmeister series; except for the acids, the cations are rather similar. (c) Surface tension of NaCl, KCl, CsCl, and NaF solutions. The points are the experimental data [5], the lines follow from the mean-field model Eq. (2) using $\varepsilon = 78$, $T = 298\,\mathrm{K}$, and $z^* = 0.5\,\mathrm{nm}$. The ionic surface affinities $\alpha_{\mathrm{Na}} = 1.2$ and $\alpha_{\mathrm{Cl}} = 1.0$ are extracted from previous simulations of the potentials of mean force of Na^+ and Cl^- at the air-water interface [34, 35]. $\alpha_{\mathrm{K}} = 1.2$, $\alpha_{\mathrm{Cs}} = 1.2$, and $\alpha_{\mathrm{F}} = 1.3$ are obtained by fits to the experimental data. The black solid line shows the model result for $\alpha_+ = \alpha_- = 0.8$ for comparison.

tials of mean force for the H_3O^+, Cl^-, Na^+, and OH^- ions [32]. Of all the ions, only H_3O^+ has a small but significant affinity for the interface, which is caused by its favorable orientation at the interface, in agreement with ab initio simulation results [32]. As shown in Fig. 2e, the simulations reproduce the experimental surface tension of NaCl, NaOH, and HCl solutions quantitatively [32]. For this the ion force fields must be very accurate, which is achieved by thermodynamic force-field optimization [34, 38]. It can be concluded that the negative surface tension of acids is indeed caused by a significant H_3O^+ affinity to the electrolyte-air interface.

JONES-RAY EFFECT

A closer look at experimental NaCl surface tension data from different labs in H_2O and D_2O (data points [39, 40]) for ultra-low electrolyte concentration in Fig. 3a is revealing. The surface tension exhibits a pronounced minimum in the concentration range of $c^{\mathrm{b}}_{\mathrm{salt}} = 0.01 - 0.001$ M, with similar results being obtained for all electrolytes [39–44]. Various explanations for this so-called Jones-Ray effect have been offered, involving instrumental wetting artifacts [45], anion adsorption [46, 47] and OH^- adsorption [48, 49], but its mechanism is still debated [35, 47, 50]. Clearly, OH^- ions cannot cause the surface tension minimum since they are repelled from the interface, as demonstrated in Fig. 1b and Fig. 2d; also the rather weak surface affinity of H_3O^+ ions is not sufficient to explain the experimental data in Fig. 3a [35]. However, the assumption of trace amounts of surface-active charged impurities allows reproduction of the Jones-Ray effect: the solid lines in Fig. 3a are modeling results for impurity concentrations in the nM range with a surface affinity of typical surfactants such as sodium dodecylsulfate (SDS) [35]. This is not unreasonable, as it is difficult to experimentally detect charged impurities at lower concentration than the inevitable water ions, which is 100 nM at neutral pH, by conductivity measurements. Thus even when using ultrapure water, purified salts, and cleaned glassware, impurities are unavoidable and have been previously invoked to explain dynamic features of air-water interfaces [51–55].

In the theoretical model used for Fig. 3, the Gibbs dividing surface is located at $z = 0$ and all ionic potentials of mean force are approximated by box profiles. The ion distribution in the water phase ($z > 0$) is assumed to follow the mean-field Poisson-Boltzmann equation

$$\varepsilon\varepsilon_0 \frac{d^2\psi(z)}{dz^2} = -e\sum_i q_i c_i^{\mathrm{b}} \mathrm{e}^{-eq_i\psi(z)/k_{\mathrm{B}}T - \alpha_i\theta(z^*-z)}, \quad (2)$$

where ε is the solution dielectric constant, ε_0 the vacuum dielectric permittivity, $\psi(z)$ the local electrostatic potential, e the elementary charge, q_i the valency of the i-th ion type, c_i^{b} the bulk concentration of the i-th ion type, $k_{\mathrm{B}}T$ the thermal energy, α_i the surface affinity of the i-th ion type, $\theta(z)$ the Heaviside function, and z^* the thickness of the surface adsorption potential. The boundary conditions for an intrinsically neutral interface are $d\psi(z)/dz|_{z=0} = 0$ and $\psi(z)|_{z\to\infty} = 0$. The ionic surface excess Γ_i is defined by $\Gamma_i = \int_0^\infty \left(c_i(z) - c_i^{\mathrm{b}}\right) dz$ where $c_i(z) = c_i^{\mathrm{b}} \mathrm{e}^{-eq_i\psi(z)/k_{\mathrm{B}}T - \alpha_i\theta(z^*-z)}$ is the local concentration of ion type i and $\psi(z)$ follows from the solution of eq. (2). Finally, the electrolyte surface tension is obtained

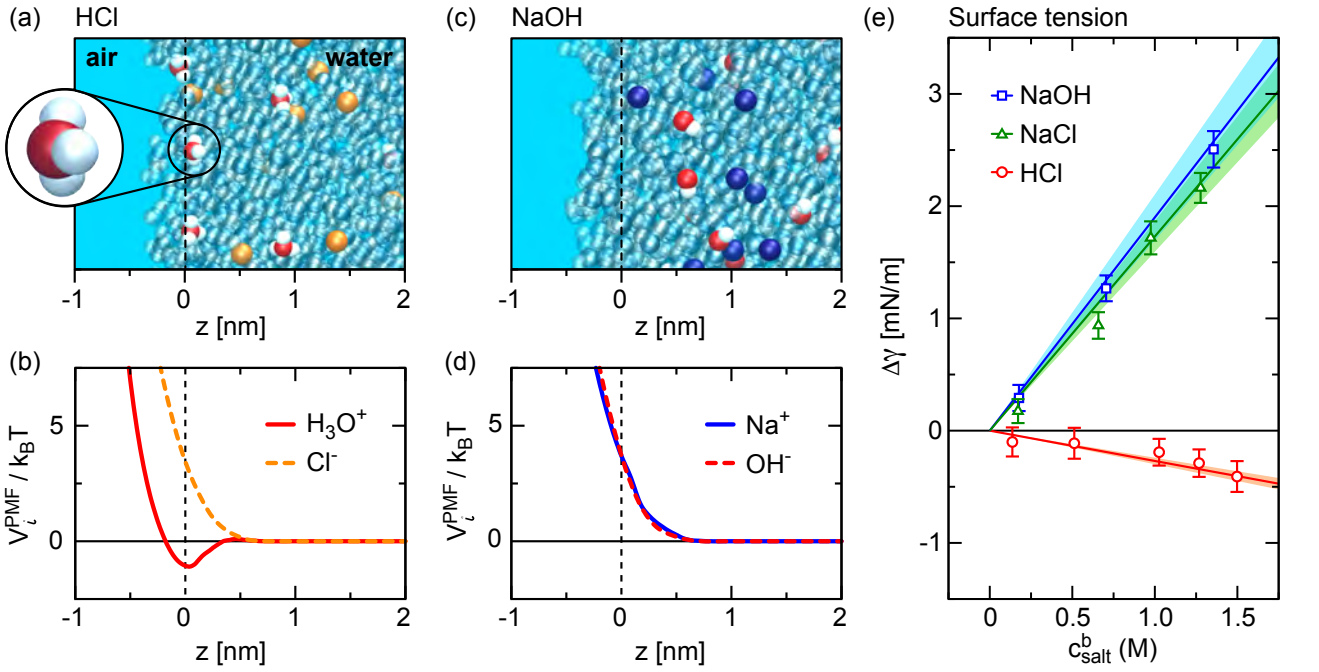

FIG. 2. (a,c) Snapshots of force-field based molecular dynamics simulations of 0.5 M HCl and NaOH solutions [32]. Oxygen and hydrogen atoms of H_3O^+ and OH^- are colored in red and white, Cl^- and Na^+ in orange and blue, respectively, water molecules are transparent. The water Gibbs dividing surface at $z = 0$ is indicated by dashed lines. H_3O^+ is weakly attracted to the interface and its favorable orientation is illustrated, whereas Cl^-, Na^+, and OH^- are depleted from the interface. (b,d) Potentials of mean force for H_3O^+, Cl^-, Na^+, and OH^- [32]. (e) Comparison of linear fits to experimental surface tension data (lines and color shaded areas which indicate the 90% confidence intervals) [4, 14] and molecular dynamics simulation results (points with error bars) [32].

by integrating Eq. (1) using the ideal-gas approximation $d\mu_i = k_BTdc_i^b/c_i^b$. For experiments in ambient air the solution pH is around 5.6 due to CO_2 dissolution [21, 56]. In the model, H_3O^+, OH^-, and HCO_3^- are included with bulk concentrations given as $c^b_{H_3O} = 10^{-pH}$ M, $c^b_{OH} = 10^{pH-14}$ M, and $c^b_{HCO_3} = c^b_{H_3O} - c^b_{OH}$. In addition, we consider impurities which completely dissociate into surface-active anions and their counterions. The surface affinities $\alpha_{Na} = 1.2$ and $\alpha_{Cl} = 1.0$ are extracted from previous simulations [34] and reproduce the experimental surface tension of NaCl in Fig. 1c. The values $\alpha_{H_3O} = -0.9$, $\alpha_{OH} = 1.6$, $\alpha_{HCO_3} = -0.4$ are taken from fits to experimental surface tension data of HCl, NaOH, and $NaHCO_3$ solutions [35], and the impurity surface affinity $\alpha_{imp} = -15.6$ is extracted from surface tension data of SDS [35].

For the modeling results in Fig. 3a the fitted impurity concentrations are $c^b_{imp} = 1.6$ nM, 18 nM, and 34 nM (black, red and blue lines) and are all well below the water ion concentration. The convincing agreement between the model results and the experimental data over the entire salt concentration range, together with the reasonable fit parameters, suggest contamination of water with surface-active charged impurities to be the cause of the Jones-Ray effect. This conclusion is corroborated by the fact that this hypothesis also explains zeta potential and disjoining pressure data, as will be explained below.

Figs. 3b and c show the impurity surface excess Γ_{imp} and the surface potential $\psi_0 = \psi(z)|_{z=0}$ as a function of the added salt concentration for the same parameters as in Fig. 3a. It is the increase of Γ_{imp} with c^b_{salt}, caused by screening of the electrostatic repulsion between adsorbed impurity molecules, which produces the minimum in the surface tension [35]. The typical surface area per impurity is of the order of 100 nm^2, in agreement with recent experimental estimates [52–54]. The adsorption of dilute impurities takes a few minutes [57], which elegantly explains why the Jones-Ray effect shows slow dynamics [43]. Interestingly, even though the impurity concentration is nano-molar, the resultant surface potential ψ_0 is substantial, in particular at low salt concentrations.

DISJOINING PRESSURE

The disjoining pressure data of a thin water film on a negatively charged silica surface (shown in Fig. 4a for different fluoride electrolytes) is positive, decays roughly exponential as a function of film thickness D and exhibits significant ion-specificity [21]. This immediately suggests that the air-electrolyte interface possesses a significant negative charge [59]. To model these data, the surface

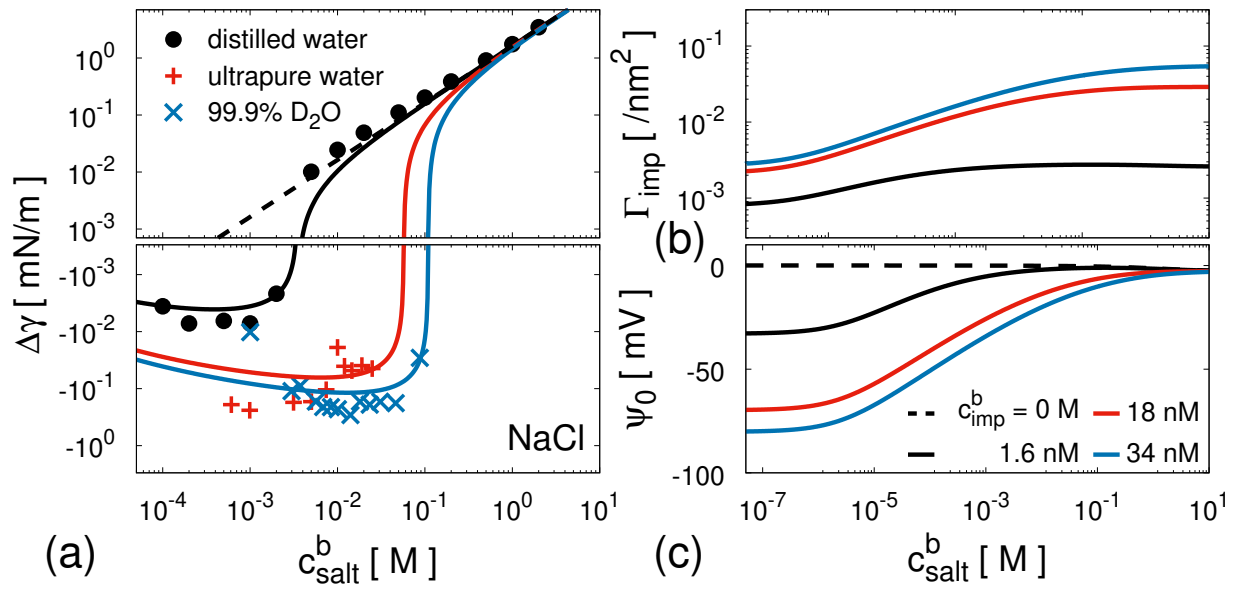

FIG. 3. (a) Surface tension increment $\Delta\gamma$ of NaCl solutions at ultra-low concentration. The black circles are the original Jones-Ray experimental data obtained by the capillary rise method [39], colored symbols are obtained by the Wilhelmy plate method in H_2O and in D_2O [40]. The lines are model predictions based on Eq. (2) in the presence of surface active H_3O^+, OH^-, HCO_3^-, charged impurities and their neutralizing counterions. Parameters used are $\varepsilon = 78$, $T = 298\,\mathrm{K}$, pH = 5.6, surface potential width $z^* = 0.5\,\mathrm{nm}$ and ionic surface affinities in units of k_BT of $\alpha_{Na} = 1.2$, $\alpha_{Cl} = 1.0$, $\alpha_{H_3O} = -0.9$, $\alpha_{OH} = 1.6$, $\alpha_{HCO_3} = -0.4$. The surface affinity of impurities $\alpha_{imp} = -15.6$ is extracted from fits to SDS experimental surface tension data [35]. The fitted impurity concentrations are $c^b_{imp} = 1.6\,\mathrm{nM}$, 18 nM, and 34 nM for the black, red, and blue solid lines, the black broken line for $c^b_{imp} = 0\,\mathrm{nM}$ is added for comparison. (b) Surface impurity excess Γ_{imp} and (c) surface potential ψ_0 as a function of the added salt concentration for the same parameters and the same impurity concentrations as in (a).

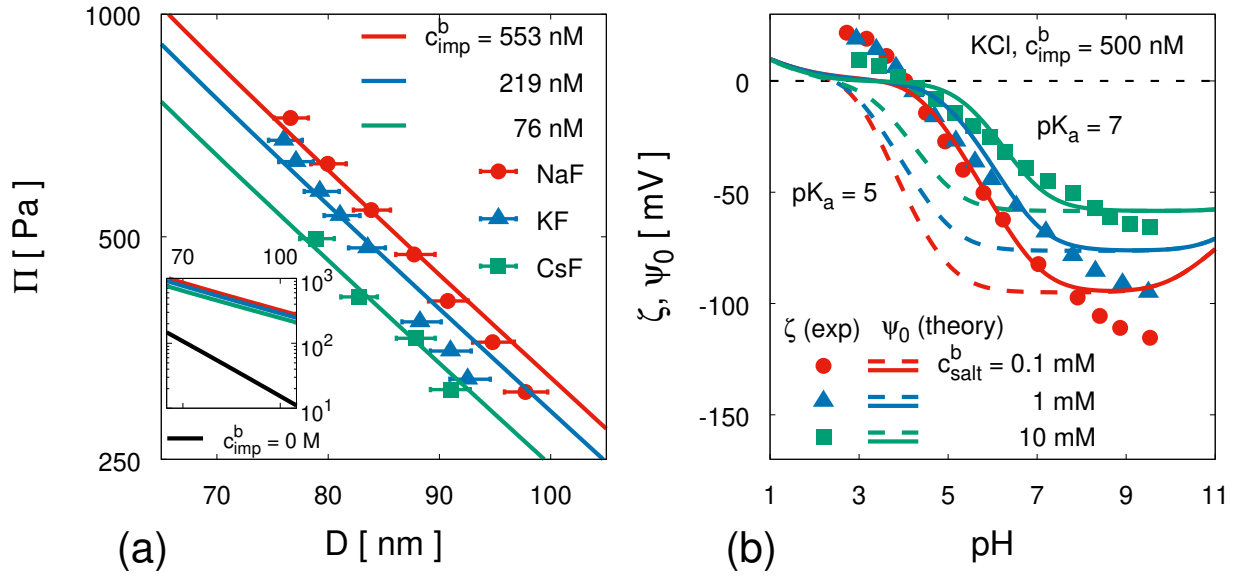

FIG. 4. (a) Disjoining pressure Π of a wetting film of 0.1 mM fluoride salt solutions on a silica surface as a function of film thickness D. Points are experimental data [21], lines are mean-field model results from Eq. (2) for fixed silica surface potential $\psi_{Si} = -135\,\mathrm{mV}$ [58]. The fitted impurity concentrations are $c^b_{imp} = 553\,\mathrm{nM}$, 219 nM, and 76 nM, for NaF, KF, and CsF solutions, respectively. Otherwise same parameters as in Fig. 3 are used. The inset shows in addition the disjoining pressure in the absence of surface-active impurities (black solid line) (b) The data points are experimental zeta potentials of hydrophobic planar polymer films for three different added KCl concentrations from Ref. 11. The lines denote mean-field model results for the surface potential from Eq. 2 in the presence of acidic charged impurities of fixed bulk concentration $c^b_{imp} = 500\,\mathrm{nM}$ with a dissociation constant of $pK_a = 5$ (broken lines) and $pK_a = 7$ (solid lines). Calculations are done in presence of surface-inactive K^+, Cl^- and OH^- ions as well as surface-active ions H_3O^+, using the same parameters as in Fig. 3.

affinities of K^+, Cs^+, and F^- ions are extracted from fits to the experimental surface tension data of NaCl, KCl, and CsCl solutions in Fig. 1c [5], resulting in the same surface affinity $\alpha_{Na} = \alpha_K = \alpha_{Cs} = 1.2$. This suggests that the cation specificity of the disjoining pressure in Fig. 4a does not originate from cation specific surface affinities. For F^- we obtain $\alpha_F = 1.3$ from the data in Fig. 1c. The model results in Fig. 4a are obtained for 0.1 mM added salt assuming pH=5.6 in the presence of H_3O^+, OH^- and HCO_3^- ions and for a fixed silica surface potential of $\psi_{Si} = -135\,\mathrm{mV}$, which is the zeta potential of silica in 0.1 mM KCl solution [58]. In the absence of charged impurities, a very small repulsive pressure is obtained (shown as a black solid line in the inset of Fig. 4a) which is due to the compression of the counterion layer at the silica surface. The fits to the experimental data yield impurity concentrations of $c^b_{imp} = 553\,\mathrm{nM}$, 219 nM, and 76 nM for NaF, KF, CsF solutions, respectively. These concentration are somewhat larger than the ones obtained for the Jones-Ray effect, but are still very dilute and not unreasonable.

ZETA POTENTIAL

Air bubbles and oil droplets in an electric field move towards the anode, which indicates a negative effective charge [10–12]. A relation between zeta potentials and the presence of impurities was fist suggested for oil droplets in water [12]; alternative mechanisms involving the surface potential of the pure air-water interface were shown to be inconsistent [60, 61]. Fig. 4b shows the experimental zeta potential of hydrophobic planar polymer films [11] as a function of pH for different concentrations of added KCl. This experimental geometry has the advantage that complications due to surface curvature are absent [62, 63]. In the experiments, the pH was adjusted by adding KOH and HCl [11]. Since the zeta potential of gas bubbles and hydrophobic surfaces is strongly pH sensitive, impurity charge regulation is included in the modeling according to $\mathrm{imp}^- + H_3O^+ \rightleftharpoons \mathrm{impH} + H_2O$, described by an acidic dissociation constant K_a. Near the interface, the impurity dissociation equilibrium is perturbed in the presence of a finite surface potential, which is fully accounted for in the model. Because the experiment was performed in nitrogen atmosphere [11], HCO_3^- is not included in the model.

Fig. 4b compares the experimental zeta potential data with the calculated surface potential ψ_0 as a function of added KCl concentration and for different pH values. The same parameters as in Fig. 3, extracted from the experimental data in Fig. 1d, are used for the interface affinities of all ions. The bulk impurity concentration for the modeling results in Fig. 4b is set to $c^b_{imp} = 500\,\mathrm{nM}$, similar to the one used in the fits to the disjoining pressure data in Fig. 4a. For an impurity dissociation constant of $pK_a = 7$ (solid lines) the model describes the experimental data better than for $pK_a = 5$ (broken lines), which points to a very weak acidic character of the impurities, even weaker than carboxyl groups, for which the experimental value of pK_a is around 5 [12, 64]. In this context it is interesting to note that pK_a values are expected to be shifted to higher values at low-dielectric surfaces [64, 65]. The experimental data in Fig. 4b exhibits an isoelectric point around pH = 4, the value of which sensitively depends on the surface type [66]. The model predicts slightly positive surface potentials for pH < 2 due to weak adsorption of H_3O^+; the larger positive experimental zeta potentials at low pH might point to the additional presence of cationic impurities.

For a hydrophobic surface as used in the experiment in Fig. 4b, the hydrodynamic boundary condition is complex and the experimentally measured zeta potential not necessarily coincides with the electrostatic surface potential [67]. In fact, the hydrodynamic boundary condition at an air-water interface depends on the presence of absorbed molecules and changes smoothly from perfect slip to no slip with rising adsorbent concentration [9, 52–54, 68–72], leading to a number of side effects [55, 68, 71]. The comparison of the experimentally measured zeta potential and the calculated electrostatic surface potential in Fig. 4b is, therefore, only tentative.

SUMMARY AND OUTLOOK

Assuming the presence of negatively charged surface-active impurities, a simple mean-field description can be used to explain a number of hitherto puzzling experimental observations, namely the presence of stable water films on silica surfaces, the observation of negative zeta potentials at hydrophobic surfaces, and finally the Jones-Ray effect. The impurity concentrations that are obtained from fits to experimental data are in the nM range, they differ for different measurement techniques and even for the same measurement done in different labs. This is not surprising, considering the different cleaning procedures and varying purity of used chemicals and lab water in different labs.

It is not clear at present what the chemical character of the impurities is, and it seems likely that experimental impurities consist of a broad mixture of different species that most likely varies from experiment to experiment. Water might become contaminated during preparation or during experiments, impurities might be present in added salts or might be ionic surfactants from detergents used for washing glassware and will most likely consist of a mixture of cationic and anionic surfactants with different surface affinities. We could explain experimental data by assuming negative impurities with a surface affinity similar to SDS; future experiments should strive to identify impurities in lab water and in chemical compounds

by modern techniques such as high performance liquid chromatography and mass spectrometry [73]. Careful experiments with added trace amounts of surfactants have already given important clues about the chemical identity of impurities [12, 54, 69–72].

Trace amounts of impurities presumably play essential roles also in other anomalies, such as the boundary dynamics of air-water interfaces [51–55], the inverse Jones-Ray effect [44, 74, 75], and the anomalous nanobubble stability [15–17]. In conclusion, the interface between electrolytes and hydrophobic surfaces is conceptually simple but in reality rather complex, since the effects of trace amounts of surfactants are amplified due to strong adsorption at the hydrophobic interface.

ACKNOWLEDGEMENTS

YU acknowledge financial supports from Grant-in-Aid for JSPS Fellows 16J00042.

REFERENCES AND RECOMMENDED READING

Papers of particular interest, published within the period of review, have been highlighted as:

- • Paper of special interest.
- •• Paper of outstanding interest.

[1] E. W. Washburn, ed., *International Critical Tables of Numerical Data, Physics, Chemistry and Technology*, electronic 1st ed., Vol. IV (Knovel, Norwich, NY, 1930) pp. 463–466.

[2] L. Onsager and N. N. T. Samaras, "The surface tension of Debye-Hückel electrolytes," J. Chem. Phys. **2**, 528–536 (1934).

[3] P. K. Weissenborn and R. J. Pugh, "Surface tension of aqueous solutions of electrolytes: Relationship with ion hydration, oxygen solubility and bubble coalescence," J. Colloid Int. Sci. **184**, 550–563 (1996).

[4] L. M. Pegram and M. T. Record, "Hofmeister salt effects on surface tension arise from partitioning of anions and cations between bulk water and the air-water interface," J. Phys. Chem. B **111**, 5411–5417 (2007).

[5] N. Matubayasi, *Surface tension and related thermodynamic quantities of aqueous electrolyte solutions* (CRC Press, 2014).

[6] Yuki Nagata, Tatsuhiko Ohto, Mischa Bonn, and Thomas D. Kühne, "Surface tension of ab initio liquid water at the water-air interface," J. Chem. Phys. **144**, 204705 (2016), • Technique to obtain interfacial tension data from ab initio simulation trajectories is developed.

[7] M. Liu, J. K. Beattie, and A. Gray-Weale, "The surface relaxation of water," J. Phys. Chem. B **116**, 8981–8988 (2012).

[8] Ines M. Hauner, Antoine Deblais, James K. Beattie, Hamid Kellay, and Daniel Bonn, "The dynamic surface tension of water," J. Phys. Chem. Lett. **8**, 1599–1603 (2017), • High precision measurements of the dynamic surface tension of water drops show slow dynamics on the millisecond timescale.

[9] N. P. Brandon, G. H. Keksall, S. Levine, and A. L. Smith, "Interfacial electrical properties of electrogenerated bubbles," J. Appl. Electrochem. **15**, 485–493 (1985).

[10] A. Graciaa, G. Morel, P. Saulner, J. Lachaise, and R. S. Schechter, "The ζ-potential of gas bubbles," J. Colloid Int. Sci. **172**, 131–136 (1995).

[11] Ralf Zimmermann, Stanislav Dukhin, and Carsten Werner, "Electrokinetic measurements reveal interfacial charge at polymer films caused by simple electrolyte ions," J. Phys. Chem. B **105**, 8544–8549 (2001), •• Negative zeta potentials of planar hydrophobic surface are measured as a function of pH and salinity.

[12] K. Roger and B. Cabane, "Why are hydrophobic/water interfaces negatively charged?" Angew. Chem. Int. Ed. **51**, 5625–5628 (2012), •• Negative zeta potential of oil droplets in water is suggested to originate from contamination of oil with fatty acids.

[13] Vincent S. J. Craig, Barry W. Ninham, and Richard M. Pashley, "The effect of electrolytes on bubble coalescence in water," J. Phys. Chem. **97**, 10192–10197 (1993).

[14] Christine L. Henry, Casuarina N. Dalton, Lehoa Scruton, and Vincent S. J. Craig, "Ion-specific coalescence of bubbles in mixed electrolyte solutions," J. Phys. Chem. C **111**, 1015–1023 (2007).

[15] William A. Ducker, "Contact angle and stability of interfacial nanobubbles," Langmuir **25**, 8907–8910 (2009).

[16] Siddhartha Das, Jacco H. Snoeijer, and Detlef Lohse, "Effect of impurities in description of surface nanobubbles," Phys. Rev. E **82**, 056310 (2010).

[17] James R. T. Seddon, Detlef Lohse, William A. Ducker, and Vincent S. J. Craig, "A deliberation on nanobubbles at surfaces and in bulk," Chem Phys Chem **13**, 2179–2187 (2012).

[18] B. V. Derjaguin and M. Kussakov, "Anomalous properties of thin polymolecular films V," Acta Physicochim. USSR **10**, 153 (1939).

[19] D. Exerowa, "Effect of adsorption, ionic strength and ph on the potential of the diffuse electric layer," Kolloid-Zeitschrift und Zeitschrift für Polymere **232**, 703–710 (1969).

[20] N.V. Churaev, "Surface forces in wetting films," Advances in Colloid and Interface Science **103**, 197–218 (2003).

[21] N. Schelero and R. von Klitzing, "Correlation between specific ion adsorption at the air/water interface and long-range interactions in colloidal systems," Soft Matter **7**, 2936 (2011), •• The repulsive disjoining pressure between the air-electrolyte interface and a silica surface is measured for different salt solutions and with high precision.

[22] Poul B. Petersen and Richard J. Saykally, "Evidence for an enhanced hydronium concentration at the liquid water surface," J. Phys. Chem. B **109**, 7976–7980 (2005), •• Non-linear surface specific spectroscopic methods are used to detect hydronium adsorption at liquid-water surfaces.

[23] Martin Mucha, Tomaso Frigato, Lori M. Levering, Heather C. Allen, Douglas J. Tobias, Liem X. Dang, and

Pavel Jungwirth, "Unified molecular picture of the surfaces of aqueous acid, base, and salt solutions," J. Phys. Chem. B 2005 **109**, 7617–7623 (2005).

[24] R. Vácha, D. Horinek, M. L. Berkowitzc, and P. Jungwirth, "Hydronium and hydroxide at the interface between water and hydrophobic media," Phys. Chem. Chem. Phys. **10**, 4975–4980 (2008).

[25] C. J. Mundy, I-F. W. Kuo, M. E. Tuckerman, H.-S. Lee, and D. J. Tobias, "Hydroxide anion at the air/water interface," Chem. Phys. Lett. **481**, 2–8 (2009).

[26] Shinichi Enami, Michael R. Hoffmann, and A. J. Colussi, "Proton availability at the air/water interface," J. Phys. Chem. Lett. **1**, 1599–1604 (2010).

[27] Himanshu Mishra, Shinichi Enami, Robert J. Nielsen, Logan A. Stewart, Michael R. Hoffmann, William A. Goddard III, and Agustn J. Colussi, "Bronsted basicity of the air-water interface," PNAS **109**, 18679–18683 (2012).

[28] M. D. Baer, I-F. W. Kuo, D. J. Tobias, and C. J. Mundy, "Toward a unified picture of the water self-ions at the air-water interface: A density functional theory perspective," J. Phys. Chem. B **118**, 8364–8372 (2014).

[29] Jochen S. Hub, Maarten G. Wolf, Carl Caleman, Paul J. van Maaren, Gerrit Groenhoff, and David van der Spoel, "Thermodynamics of hydronium and hydroxide surface solvation," Chem. Sci. **5**, 1745 (2014).

[30] T. T. Duignan, D. F. Parsons, and B. W. Ninham, "Hydronium and hydroxide at the air-water interface with a continuum solvent model," Chem. Phys. Lett. **635**, 1–12 (2015).

[31] Y-L. S. Tse, C. Chen, G. E. Lindberg, R. Kumar, and G. A. Voth, "Propensity of hydrated excess protons and hydroxide anions for the air-water interface," J. Am. Chem. Soc. **137**, 12610–12616 (2015).

[32] S. Mamatkulov, C. Allolio, R. R. Netz, and D. J. Bonthuis, "Orientation induces adsorption of the hydrated proton at the air-water interface," Angew. Chem. Int. Ed. **56**, 15846–15851 (2017), • Hydronium adsorption at air-electrolyte interfaces is explained by favorable orientation of its dipole by using force-field molecular dynamics simulation with optimized force fields.

[33] X. Yan, M. Delgado, J. Aubry, O. Gribelin, A. Stocco, F. Boisson-Da Cruz, J. Bernard, and F. Ganachaud, "Central role of bicarbonate anions in charging water/hydrophobic interfaces," J. Phys. Chem. Lett. **9**, 96–103 (2018).

[34] D. Horinek, A. Herz, L. Vrbka, F. Sedlmeier, S. I. Mamatkulov, and R. R. Netz, "Specific ion adsorption at the air/water interface: The role of hydrophobic solvation," Chem. Phys. Lett. **479**, 173–183 (2009).

[35] Y. Uematsu, D. J. Bonthuis, and R. R. Netz, "Charged surface-active impurities at nanomolar concentration induce Jones-Ray effect," J. Phys. Chem. Lett. **9**, 189–193 (2018), • The Jones-Ray effect is quantitatively explained by assuming surface-active charged impurity at nanomolar concentration.

[36] Nadine Schwierz, Dominik Horinek, Uri Sivan, and Roland R. Netz, "Reversed Hofmeister series - the rule rather than the exception," Current Opinion in Colloid and Interface Science **23**, 10–18 (2016).

[37] Pavel Jungwirth, "Ions at aqueous interfaces," Faraday Discuss. **141**, 9–30 (2009).

[38] Douwe Jan Bonthuis, Shavkat I. Mamatkulov, and Roland R. Netz, "Optimization of classical nonpolarizable force fields for OH^- and H_3O^+," J. Chem. Phys **144**, 104503 (2016).

[39] G. Jones and W. A. Ray, "The surface tension of solutions of electrolytes as a function of the concentration iii. sodium chloride," J. Am. Chem. Soc. **63**, 3262–3263 (1941).

[40] Yixing Chen, Halil I. Okur, Nikolaos Gomopoulos, Carlos Macias-Romero, Paul S. Cremer, Poul B. Petersen, Gabriele Tocci, David M. Wilkins, Chungwen Liang, Michele Ceriotti, and Sylvie Roke, "Electrolytes induce long-range orientational order and free energy changes in the H-bond network of bulk water," Sci. Adv. **2**, e1501891 (2016).

[41] G. Jones and W. A. Ray, "The surface tension of solutions of electrolytes as a function of the concentration. I. a differential method for measuring relative surface tension," J. Am. Chem. Soc. **59**, 187–198 (1937), •• First experimental report of a surface tension minimum of electrolyte solutions as a function of salt concentration.

[42] M. Dole and J. A. Swartout, "A twin-ring surface tensiometer. I. the apparent surface tension of potassium chloride solutions," J. Am. Chem. Soc. **62**, 3039–3045 (1940).

[43] G. Passoth, "Uber den Jones-Ray-Effekt und die Oberflächenspannung verdünnter Elektrolytlosungen," Z. Physik. Chem. **211O**, 129–147 (1959).

[44] J. E. B. Randles and D. J. Schiffrin, "Surface tension of dilute acid solutions," Trans. Faraday Soc. **62**, 2403–2408 (1966).

[45] I. Langmuir, "Repulsive forces between charged surfaces in water and the cause of the jones-ray effect," Science **88**, 430–432 (1938).

[46] M. Dole, "A theory of surface tension of aqueous solutions," J. Am. Chem. Soc. **60**, 904–911 (1938).

[47] P. B. Petersen and R. J. Saykally, "Adsorption of ions to the surface of dilute electrolyte solutions: The Jones-Ray effect revisited," J. Am. Chem. Soc. **127**, 15446–15452 (2005).

[48] K. A. Karraker and C. J. Radke, "Disjoining pressures, zeta potentials and surface tensions of aqueous non-ionic surfactant electrolyte solutions: theory and comparison to experiment," Adv. Colloid Int. Sci. **96**, 231–264 (2002).

[49] M. Manciu and E. Ruckenstein, "Specific ion effects via ion hydration: I. surface tension," Adv. Colloid Int. Sci. **105**, 63–101 (2003).

[50] H. I. Okur, Y. Chen, D. M. Wilkins, and S. Roke, "The jones-ray effect reinterpreted: Surface tension minima of low ionic strength electrolyte solutions are caused by electric field induced water-water correlations," Chem. Phys. Lett. **684**, 433–442 (2017).

[51] José A. Nicolás and José M. Vega, "A note on the effect of surface contamination in water wave damping," J. Fluid Mech. **410**, 367–373 (2000).

[52] Ofer Manor, Ivan U. Vakarelski, Xiaosong Tang, Sean J. OShea, Geoffrey W. Stevens, Franz Grieser, Raymond R. Dagastine, and Derek Y. C. Chan, "Hydrodynamic boundary conditions and dynamic forces between bubbles and surfaces," Phys. Rev, Lett **101**, 024501 (2008).

[53] Ofer Manor, Ivan U. Vakarelski, Geoffrey W. Stevens, Franz Grieser, Raymond R. Dagastine, and Derek Y. C. Chan, "Dynamic forces between bubbles and surfaces and hydrodynamic boundary conditions," Langmuir **24**, 11533–11543 (2008).

[54] A. Maali, R. Boisgard, H. Chraibi, Z. Zhang, H. Kellay, and A. Würger, "Viscoelastic drag forces and crossover from no-slip to slip boundary conditions for flow near air-water interfaces," Phys. Rev. Lett. **118**, 084501 (2017), •• The presence of impurities at the air-water interface is concluded from dynamic AFM measurements at bubbles.

[55] M. Arangalage, X. Li, F. Lequeux, and L. Talini, "Dual Marangoni effects and detection of traces of surfactants," Soft Matter **14**, 3378 (2018).

[56] A. Persat, R. D. Chambers, and J. G. Santiago, "Basic principles of electrolyte chemistry for microfluidic electrokinetics. part i: Acid/base equilibria and ph buffers," Lab on a Chip **9**, 2437–2453 (2009).

[57] Chaodong Yang and Yongan Gu, "Modeling of the adsorption kinetics of surfactants at the liquid-fluid interface of a pendant drop," Langmuir **20**, 2503–2511 (2004).

[58] Grinnell Jones and Lloyd A. Wood, "The measurement of potentials at the interface between vitreous silica and solutions of potassium chloride by the streaming potential method," J. Chem. Phys. **13**, 106 (1945).

[59] Sven Holger Behrens and Michal Borkovec, "Exact poisson-boltzmann solution for the interaction of dissimilar charge-regulating surfaces," Phys Rev E **60**, 7040–7048 (1999).

[60] Douwe Jan Bonthuis, Dominik Horinek, Lyderic Bocquet, and Roland R. Netz, "Electrohydraulic power conversion in planar nanochannels," Phys. Rev. Lett. **103**, 144503 (2009).

[61] D. J. Bonthuis, K. Falk, C. N. Kaplan, D. Horinek, A. N. Berker, L. Bocquet, and R. R. Netz, "Comment on "pumping of confined water in carbonnanotubes by rotation-translation coupling"," Phys. Rev. Lett. **105**, 209401 (2010).

[62] D. C. Henry, "The cataphoresis of suspended particles. part i. the equation of cataphoresis," Proc. R. Soc. London, Ser. A **133**, 106 (1931).

[63] R. W. O'Brien and L. R. White, "Electrophoretic mobility of a spherical colloidal particle," J. Chem. Soc., Faraday Trans. 2 **74**, 1607 (1978).

[64] Bethany A. Wellen, Evan A. Lach, and Heather C. Allen, "Surface pka of octanoic, nonanoic, and decanoic fatty acids at the air-water interface: applications to atmospheric aerosol chemistry," Phys. Chem. Chem. Phys. **19**, 26551–26558 (2017).

[65] R. R. Netz, "Charge regulation of weak polyelectrolytes at low- and high-dielectric-constant substrates," J. Phys.: Condens. Matter **15**, S239–S244 (2003).

[66] Thomas W. Healy and Douglas W. Fuerstenau, "The isoelectric point/point-of zero-charge of interfaces formed by aqueous solutions and nonpolar solids, liquids, and gases," Journal of Colloid and Interface Science **309**, 183–188 (2007).

[67] Douwe Jan Bonthuis and Roland R. Netz, "Unraveling the combined effects of dielectric and viscosity profiles on surface capacitance, electro-osmotic mobility, and electric surface conductivity," Langmuir **28**, 16049–16059 (2012).

[68] Derek Y. C. Chan, Evert Klaseboer, and Rogerio Manica, "Film drainage and coalescence between deformable drops and bubbles," Soft Matter **7**, 2235–2264 (2011).

[69] Laurent Joly, François Detcheverry, and Anne-Laure Biance, "Anomalous ζ potential in foam films," Phys. Rev. Lett. **113**, 088301 (2014).

[70] Alexia Barbosa De Lima and Laurent Joly, "Electroosmosis at surfactant-laden liquid-gas interfaces: beyond standard models," Soft Matter **13**, 3341–3351 (2017).

[71] Oriane Bonhomme, Baptiste Blanc, Laurent Joly, Christophe Ybert, and Anne-Laure Biance, "Electrokinetic transport in liquid foams," Adv. Colloid Int. Sci. **247**, 477–490 (2017).

[72] Baptiste Blanc, Oriane Bonhomme, Pierre-Francois Brevet, Emmanuel Benichou, Christophe Ybert, and Anne-Laure Biance, "Electroosmosis near surfactant laden liquid-air interfaces," Soft Matter **14**, 2604–2609 (2018).

[73] Tarun Anumol, Sylvain Merel, Bradley O. Clarke, and Shane A. Snyder, "Ultra high performance liquid chromatography tandem mass spectrometry for rapid analysis of trace organic contaminants in water," Chemistry Central Journal **7**, 104 (2013).

[74] Philip B. Lorenz, "The specific adsorption isotherms of thiocyanate and hydrogen ions at the free surface of aqueous solutions," J. Phys. Chem. **54**, 685–690 (1950).

[75] J. K. Beattie, A. M. Djerdjev, A. Gray-Weale, N. Kallay, J. Lützenkirchen, T. Preočanin, and A. Selmani, "ph and the surface tension of water," J. Colloid and Int. Sci. **422**, 54–57 (2014).